Journal of the Serbian Chemical Society
JSCS@tmf.bg.ac.rs • www.shd.org.rs/JSCS

J. Serb. Chem. Soc. *88* (1) 25–39 (2023)
JSCS–5608

Original scientific paper
Published 14 December 2022

Design of benzimidazoles, benzoxazoles, benzothiazoles and thiazolopyridines as leukotriene A_4 hydrolase inhibitors through 3D-QSAR, docking and molecular dynamics

MARCOS LORCA[1], MARIO FAÚNDEZ[2], C. DAVID PESSOA-MAHANA[2], GONZALO RECABARREN-GAJARDO[2,3], BENJAMIN DIETHELM-VARELA[2], DANIELA MILLÁN[4], ISMAIL CELIK[5], MARCO MELLADO[6], ILEANA ARAQUE[1], JAIME MELLA[1,7]* and JAVIER ROMERO-PARRA[8]**

[1]*Institute of Chemistry and Biochemistry, Faculty of Science, University of Valparaíso, Valparaíso 2360102, Chile,* [2]*Faculty of Chemistry and Pharmacy, Pontifical Catholic University of Chile, Santiago 7820436, Chile,* [3]*Interdisciplinary Center for Neurosciences, Pontifical Catholic University of Chile, Santiago 8330024, Chile,* [4]*Integrative Center for Biology and Applied Chemistry, Bernardo O'Higgins University, Santiago 8370854, Chile,* [5]*Department of Pharmaceutical Chemistry, Faculty of Pharmacy, Erciyes University, Kayseri 38039, Turkey,* [6]*Instituto de Investigación y Postgrado, Facultad de Ciencias de la Salud, Universidad Central de Chile, Santiago 8330507, Chile,* [7]*Chilean Pharmacopeia Research Center, University of Valparaíso, Valparaíso 2360134, Chile and* [8]*Department of Organic Chemistry and Physical Chemistry, Faculty of Chemistry and Pharmaceutical Sciences, University of Chile, Santiago 8380544, Chile*

(Received 27 April, revised 1 August, accepted 18 August 2022)

Abstract: Human leukotriene A_4 hydrolase enzyme (LTA_4H) catalyses the biotransformation of the inactive precursor leukotriene A_4 (LTA_4) to the bioactive Leukotriene B_4 (LTB_4), which causes many inflammatory responses in the human body. Therefore, the selective inhibition of this enzyme becomes a useful strategy for the treatment of several illnesses such as asthma, allergic rhinitis, cardiovascular diseases, and cancer. Herein we report a 3D-QSAR/ /CoMFA and CoMSIA study on a series of 47 benzimidazoles, benzoxazoles, benzothiazoles and thiazolopyridines reported as potent LTA_4H inhibitors. Good statistical parameters were obtained for the best model (q^2 = 0.568, r^2_{ncv} = 0.891 and r^2_{test} = 0.851). A new series of 10 compounds capable of inhibiting leukotriene A_4 hydrolase with high potency was presented. All designed inhibitors showed low IC_{50} in nano- and sub-nanomolar ranges, when they were evaluated in 3D-QSAR models. Subsequently, the designed molecules, as well as the least and most active compounds were subjected to docking and molecular dynamics studies into LTA_4H. In conclusion, we summarised a thorough structure–activity relationship (SAR) of LTA_4H inhibitors of

* Corresponding authors. E-mail: (*)jaime.mella@uv.cl; (**)javier.romero@ciq.uchile.cl
https://doi.org/10.2298/JSC220427068L

heterocyclic structure. These models can be used for the rational proposal of new inhibitors.

Keywords: CoMFA; CoMSIA; binding free energy calculation; CADD; inflamemation; allergy.

INTRODUCTION

Leukotrienes (LTs) are lipid mediators synthesised primarily in leukocytes (mast cells, eosinophils, basophils, macrophages and so on).[1] The imbalance in the biosynthesis or metabolism of LTs is associated with inflammatory processes, asthma, cardiovascular diseases, chronic obstructive pulmonary disease (COPD), and cancer.[2] LTA_4 is the common inactive precursor that produces the bioactive leukotrienes by Human LTA_4 Hydrolase enzyme (LTA_4H). Given the importance of LTA_4H, obtaining novel and potent LTA_4H inhibitors is useful to treat various inflammatory diseases. Nowadays there is only a few drugs with the ability to modulate the leukotriene system, such as zileuton, zafirlukast and montelukast.[3]

Currently a number of LTA_4H inhibitors with several chemotypes different than heterocycles have been described, Kelatorphan is an example of these[4] (Fig. 1). Other relevant compounds are JNJ-26993135 and the thiazolopyridine JNJ--40929-837 developed by Johnson & Johnson Pharmaceutical Research (Fig. 1).[5,6]

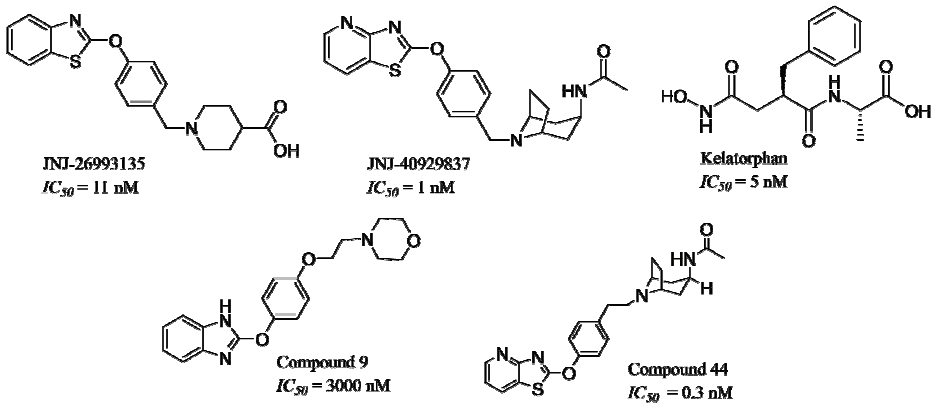

Fig. 1. Leukotriene A_4 hydrolase inhibitors. Kelatorphan represents a different class of non-heterocyclic inhibitor (*N*-hydroxyamide), whereas JNJ-26993135 and JNJ-40929837 are heterocyclic inhibitors developed by Johnson & Johnson Pharmaceutical Research. The least (**9**) and most active (**44**) compounds of the study are also displayed.

Pontiki *et al.* have reviewed some QSAR works on 5-LO inhibitors.[7] Bernstein[8] performed a QSAR of different antagonists of the cysteinyl leukotriene receptors (cysLT). Likewise, Sonawane *et al.*[9] built a QSAR of a series of phenylmethylphenoxypropylamino propanoic acid derivatives, and Sundarapandian *et*

al.[10] published a QSAR study of 142 compounds with substantial chemical diversity. Nevertheless, in none of them were applied a three-dimensional quantitative structure–activity relationship (3D-QSAR), comparative molecular field analysis (CoMFA) and comparative molecular similarity index analysis (CoMSIA) models. Accordingly, to date, no 3D-QSAR reports of any specific heterocyclic LTA_4H inhibitors are available.

In this study, we have compiled a series of 47 reported benzimidazoles, benzoxazoles, benzothiazoles and thiazolopyridines developed by Johnson & Johnson Pharmaceutical Research.[5,11,12] We performed a robust statistical 3D-QSAR of these large series of heterocyclic compounds to obtain a rational design and synthesis of promising new molecules through a CoMFA and CoMSIA. Later, we proposed a design of 10 new molecules as LTA_4H inhibitors (**1x**–**10x**). Furthermore, these 10 proposed compounds in conjunction with the most and least active inhibitors of the series (the compounds **9** and **44**) were subjected to docking and molecular dynamics assays over the human LTA_4H (PDBID:3FTS),[13] finding the agreement between 3D-QSAR and docking studies. All proposed designed compounds showed good inhibitory activities in a low and sub nanomolar range.

EXPERIMENTAL

Data selection and LTA_4H inhibitory activity

CoMFA and CoMSIA studies were performed on a set of 47 different heterocycles reported by Johnson & Johnson Pharmaceutical Research[5,11,12] (Table S-I, Supplementary material to this paper). Compounds were randomly divided into training and test sets. The distribution of pIC_{50} values for the complete set are shown in Fig. S-1 (Supplementary material). In all cases, the biological activity followed a Gaussian distribution where most compounds lie in the pIC_{50} range between 5.5 and 9.5.

CoMFA and CoMSIA calculations

CoMFA and CoMSIA studies were performed with Sybyl X-1.2 software. To derive the CoMFA and CoMSIA descriptor fields, the aligned molecules (Fig. S-2, Supplementary material) were subjected to the standard protocol, as it has been previously published by our research group.[14] PLS analysis was used to construct a linear correlation between the CoMFA and CoMSIA descriptors (independent variables) and the activity values (dependent variables). To select the best model, the cross-validation analysis was performed using the leave-one-out (LOO) method. Furthermore, the external predictive power of the developed 3D-QSAR models using the test set was examined by considering r^2_{test} and r^2_m. To confirm that the results are not obtained by a chance correlation, the Y-random test was carried out. Finally, the applicability domain (AD) was evaluated based on the simple standardisation method reported by Roy *et al.*[15]

Docking and molecular dynamics calculations

The molecular docking was performed according to the standard protocols as it is reported by our group using the leukotriene A_4 hydrolase PDBID:3FTS[14] in Autodock 4.2. The zinc atom was designated as the centre of the grid. The volumes chosen for the grid maps

were made up of 60×60×60 points, with a grid-point spacing of 0.0375 nm. The results were visualised in Visual molecular dynamics program (VMD).

Molecular dynamics simulation was performed with Gromacs 2020.4 version (Groningen machine for chemical simulations) to examine the leukotriene A_4 hydrolase – compound **7x**, **9x** and **10x** complexes stability. The molecular dynamics system input files were created following the same standard protocol reported by our group. Graphs were generated with GraphPad Prism. The binding free energy calculation by molecular mechanics Poisson–Boltzmann surface area (MM-PBSA) was performed between 80 and 100 ns using RashmiKumari's g_mmpbsa packages.[16] The average binding free energy was calculated using the "MmPbSaStat" Python script provided in "g_mmpbsa".

RESULTS AND DISCUSSION

Contour maps analysis and docking results

For the description and analysis of the CoMFA and CoMSIA contour maps, the least and the most active compounds of the series were used as a template (**9** and **44**, respectively). Both molecules are shown in Figs. 2 and 3 surrounded by different coloured polyhedrons, which represent the electrostatic, steric, hydrophobic, and hydrogen-bond donor–acceptor fields. The main interactions found in the docking studies are discussed along this section.

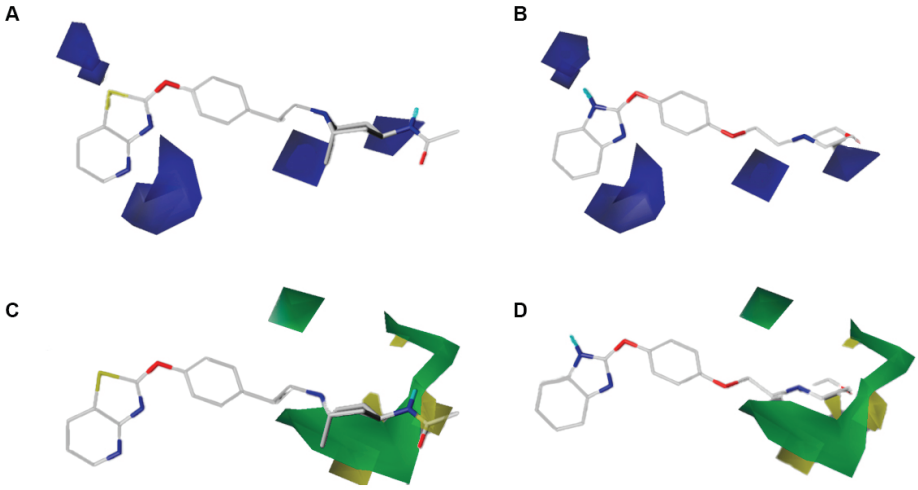

Fig. 2. CoMFA electrostatic (A and B) and steric (C and D) contour maps around compounds **44** (A and C) and **9** (B and D), the most active and less active of the series, respectively.

CoMFA electrostatic and steric contour maps

The electrostatic contour map shows two blue polyhedrons far from position 1, 3, and 4 of each heterocyclic cores of the compounds **9** and **44** (Fig. 2A and B). The incorporation of chains which contain electron-deficient atoms or groups projected toward that zone could favour the inhibitory activity over the enzyme. Even though all LTA_4H inhibitors shown in Table S-I (the compounds **1**–**47**) pos-

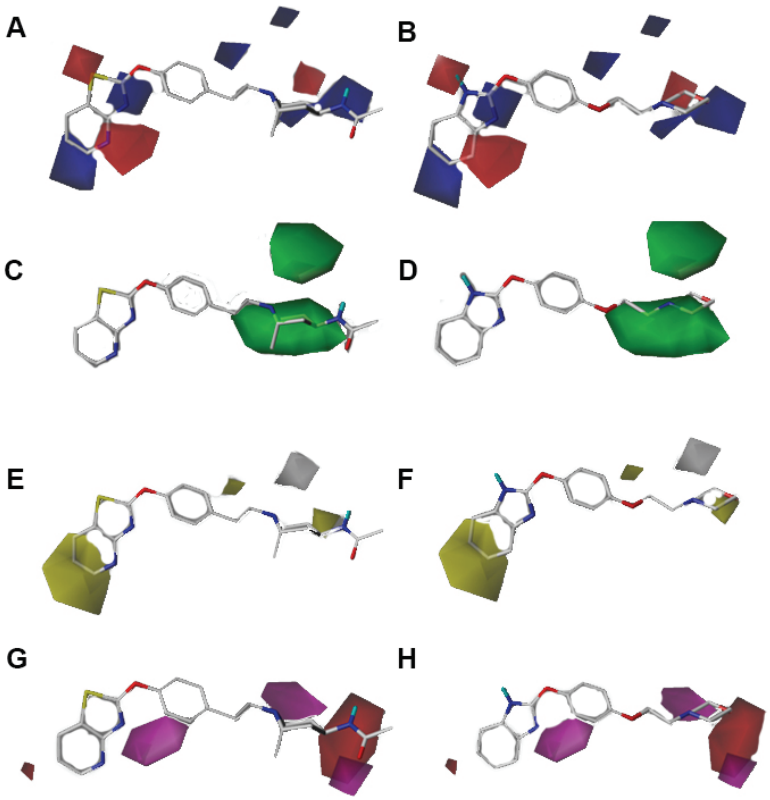

Fig. 3. CoMSIA electrostatic (A and B), steric (C and D), hydrophobic (E and F) and acceptor (G and H) contour maps around compounds **44** (A, C, E and G) and **9** (B, D, F and H), the most active and less active of the series, respectively.

sess electronegative atoms, such as sulphur, nitrogen or oxygen in their aromatic heterocyclic moieties, these are incapable of reaching contact with the blue polyhedrons mentioned above. In fact, the evidence demonstrates that these heteroatoms grant good inhibitory activities in all compounds. Considering this information, sulphur and nitrogen atoms were incorporated at positions 1 and 3, respectively, of all thiazolopyridine rings in the proposed compounds **1x**–**10x** (see Fig. 4). Furthermore, the latter were corroborated by our docking studies, where a hydrogen bond interaction can be seen between the hydroxyl group of Tyr378 and the sp^2 nitrogen atom at position 3 of the compounds **9**, **44**, **1x** and **3x**–**6x**, (Fig. S-3, Supplementary material). It should be noted that the hydrogen bond interaction described with Tyr378 can be confirmed at the hydrogen bond acceptor contour map of the CoMSIA model (see below). The compounds **2x**, **7x** and **8x** did not show this hydrogen bond interaction due to their heterocyclic thiazolopyridine rings being inverted into the catalytic site of the LTA_4H (Fig. S-3, Supplementary material).

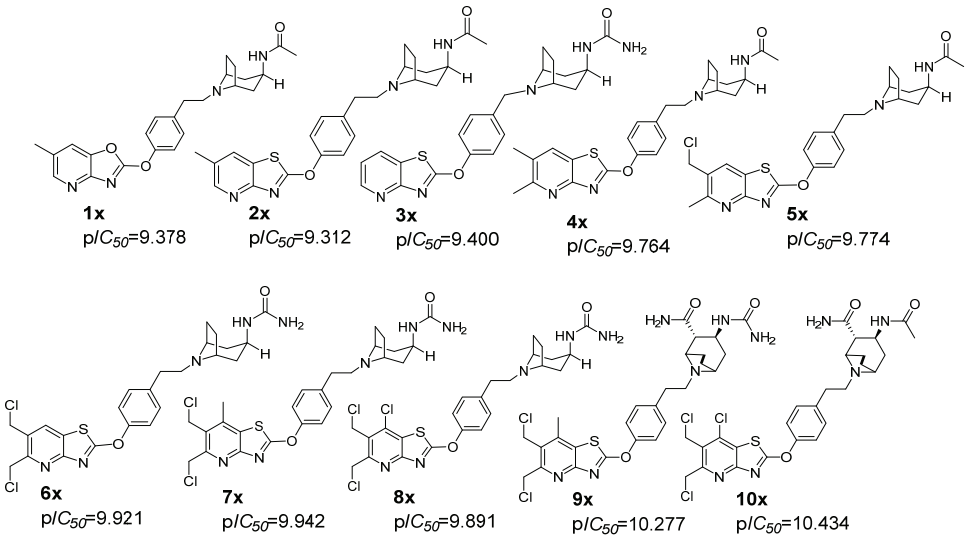

Fig. 4. Proposed structures of new molecules and their predicted pIC_{50} values.

A blue polyhedron can be seen intersecting the nitrogen atom in the amide group of the most active compound **44** (Fig. 2A) indicating that the amide function, and especially the hydrogen atom, would be favourable. This is corroborated by the high inhibitory activity that the compound **47** shows, with a pIC_{50} = = 9.000. The proposed designed structures **1x**–**10x** of Fig. 4 bear amide or urea groups, which is in line with these results. In addition, docking studies revealed that the structures **44** and **1x**–**9x** (except **10x**) showed a hydrogen bond interaction between the amides or urea groups and the carboxylate of amino acid Glu384, suggesting that they are the important functions for the inhibition of LTA_4H.

On the other hand, the less active compound **9** (Fig. 2B) shows its oxygen atom of the aliphatic morpholine ring projected towards the polyhedron, which would explain the lower inhibitory activity of this derivative. Docking assays have shown a hydrogen bond interaction between the oxygen of the morpholine ring and the Lys565 residue of the enzyme. However, this bond would not be enough to grant a good biological activity. In fact, those derivatives that have shown that the lowest inhibitory profiles, such as the compound **8** (pIC_{50} = = 6.456) bear an electron-rich oxygen group projected towards this blue polyhedron. This data was considered for the proposal of the designed compounds, establishing a functional amide or urea group in the vicinity of the blue polyhedron, which achieves an interaction with Glu384 of the catalytic site of LTA_4H.

The steric contour map (Figs. 2C and D) shows a large green polyhedron surrounding the cycloalkyl portions of the compounds **9** and **44**, meaning that

large rings or bulky groups at this part of the molecules would be beneficial for biological activity. As can be seen from Table S-I, the most active compounds, **44** and **47,** have a bulky azabicyclooctane ring in their structures, whereas the least active compounds (**9**, **34** and **35**) have less bulky rings, such as morpholine or piperidine. Considering this, the new molecules proposed **1x**–**10x** (Fig. 4), were designed maintaining the azabicyclooctane ring on their structures. Additionally, particularly in the derivatives **9x** and **10x,** a new amide group was added into the azabicyclooctane with the aim of increasing the volume and performing a hydrogen bond interaction through the oxygen atom of the amide with Lys565 of the enzyme. It is worth mentioning that more distant yellow polyhedrons surrounding the green regions are observed, which suggests a restriction of increasing the volume in this area.

CoMSIA electrostatic, steric, hydrophobic and hydrogen-bond acceptor contour maps

On the electrostatic map (Fig. 3A and B) it can be seen, unlike in the CoMFA in Fig. 2, a red polyhedron intersecting the sulphur and nitrogen atoms (or carbon atom in benzimidazole) at positions 1 and 4 of the thiazolopyridine and benzimidazole rings in the compounds **44** and **9,** respectively. This suggests that the electronegative atoms at those positions could be beneficial for the inhibitory activity. This explains why the most active compounds (**33**, **44** and **47**) exhibit sulphur atoms at position 1 and a nitrogen atom at position 4 in their aromatic heterocyclic cores, whereas the less active compounds (**9** and **15**) exhibit a nitrogen atom at position 1 (NH chemical group) and a carbon atom at position 4. It is noteworthy that thiazolopyridines, in contrast to benzimidazole, benzoxazole and benzothiazole inhibitors, showed the best inhibitory activities, which could be attributed to the nitrogen atom at position 4 of the heterocyclic framework. The latter is the reason why we have not considered the design of benzimidazoles in our proposed structures shown in Fig. 4.

Considering the well predicted pIC_{50} of designed compounds **1x**–**10x**, it could be a consequence of each one of them being thiazolopyridines bearing a nitrogen atom at position 4. In addition, is possible that this pyridine nitrogen atom of the thiazolopyridine ring could be involved, in some derivatives, in carrying out a π–π interaction with the amino acid Tyr383, as was demonstrated by our docking studies for the proposed derivatives **9x** and **10x** (Fig. S-3, Supplementary material), with these compounds having the best predicted pIC_{50} values (10.277 and 10.434, respectively). This could be explained because the Tyr383 residue has a hydroxyl group, which donates its electron density via resonance to the conjugated phenyl system, stimulating the π–π interaction with the pyridine ring of the thiazolopyridines, which have a low electron density in the presence of the nitrogen atom.

Positions 5 and 6 of the aromatic heterocycles of **9** and **44** in the electrostatic contour map (Figs. 3A and 3B)3 show a blue polyhedron nearby, indicating that the electropositive atoms projected to that region could be favourable for the inhibitory activity. For this reason, in the design of the proposed compounds shown in Fig. 4, chloromethylene groups on derivatives **5x**–**10x** were incorporated at those positions, leading to good pIC_{50} values due to the addition of electronegative atoms (chlorine) adjacent to the methylene carbons.

On the other hand, a blue polyhedron, analogous to one observed previously in the CoMFA analysis, surrounded the nitrogen atom of the amide in the compound **44** and the oxygen atom of the morpholine in the compound **9** (Figs. 3A and B, respectively). This emphasises that the presence of urea, amide or similar chemical group in this region could perform an interaction with Glu384 of the catalytic site of the enzyme.

The CoMSIA steric contour map (Figs. 3C and D) shows a similar situation as in the CoMFA analysis. Two green polyhedrons are surrounding the cycloalkyl portions of compounds **9** and **44**, which implies that bulky rings are preferred instead of planar rings or low bulky groups (see also the CoMFA steric contour map in Figs. 2C and D).

As can be seen in Figs. 3E and F, the hydrophobic contour map displays yellow polyhedral surfaces intersecting positions 5, 6 and 7 of the benzimidazole and thiazolopyridine rings in compounds **9** and **44**. The latter means that the increasing lipophilicity on those positions of the heterocyclic rings would be beneficial for the inhibitory activity. Therefore, this suggests that the insertion of methyl, halogen or alkyl-halogen groups could be a good strategy to increase the inhibitory activity over LTA_4H. Consequently, the proposed compounds **1x**, **2x** and **4x**–**10x** were designed while considering the functional groups mentioned above; thus, they bear those groups on their structures and show good predicted pIC_{50} values.

Furthermore, a small yellow polyhedron laying close to the oxygen atom of morpholine ring in compound **9** can be seen in Fig. 3F. This result means that the presence of polar hydrophilic atoms at that position would be detrimental for the inhibitory activity, which would explain some of the reasons for the reduced ability to inhibit the LTA_4H showed by **9** in comparison with the other compounds tested by Johnson & Johnson Pharmaceutical Research.[5,11,12]

On this contour map, magenta and red polyhedral surfaces can be seen (Figs. 3G and H). Magenta polyhedrons indicate that the presence of hydrogen bond acceptor groups is favourable for the biological activity, whereas the red polyhedrons indicate that hydrogen bond acceptor groups is unfavourable. A magenta polyhedron is nearby to the nitrogen atom at position 3 of the benzimidazole and thiazolopyridine rings in the compounds **9** and **44**, respectively (Figs. 3G and H), suggesting that an unprotonated nitrogen atom on that position would be appro-

priate. This would explain the low inhibitory activity showed by the benzimidazole derivatives such as **3**, **6**, **9** or **15**. The benzimidazole ring shows a tautomerism phenomenon between the nitrogen atoms at positions 1 and 3 of the heterocyclic system; therefore, the hydrogen atom, which is initially on the nitrogen 1, is constantly moving between both heteroatoms at positions 1 and 3 in the benzimidazole core. For this reason, we have dismissed the presence of the benzimidazole framework from the design of the novel derivatives **1x**–**10x** (Fig. 4), proposing only thiazolopyridine derivatives, which bear a sp^2 nitrogen atom at position 3, and show low basicity properties. as they remained unprotonated at physiological conditions. In addition, as we already have analysed for the CoMFA-electrostatic contour maps (see above), and considering the obtained results from docking assays, the magenta polyhedron nearby to the nitrogen atom at position 3 of the heterocycles agrees with the hydrogen bond interaction showed between the hydroxyl group of Tyr378 and this nitrogen atom at position 3. This corroborates the correlation between our 3D-QSAR models, and the docking experiments performed.

Another magenta polyhedron can be seen close to the azabicyclooctane ring of the compound **44** and to the morpholine scaffold of the compound **9** (Figs. 3G and H), suggesting that the insertion of hydrogen bond acceptor groups on this core could be favourable for biological activity. Taking this into account, the compounds **9x** and **10x** in Fig. 4 were designed bearing an extra amide group in the azabicyclooctane framework, resulting in being the most active compounds with the highest predicted pIC_{50} values of 10.277 and 10.434, respectively) when they were evaluated in the 3D-QSAR models. As was already mentioned above at the CoMFA-steric contour map, the amide groups in **9x** and **10x** perform hydrogen bond interactions through the carbonyl oxygen of the amides and the protonated amine of Lys565 (NH_3^+), supporting the favourability of hydrogen bond acceptors groups at this area.

Finally, there is a magenta polyhedral surface adjacent to the carbonyl oxygen atom of the amide group at the position 4 of the azabicyclooctane ring in the compound **44** (Fig. 3G). This suggests that a carbonyl group is highly favourable for the enzymatic inhibitory activity. Furthermore, there is also a red polyhedron near the nitrogen atom of the amide group in the derivative **44**. Likewise, the same polyhedron is represented close to the oxygen atom of the morpholine group in the compound **9** (Fig. 3H). Therefore, the presence of a hydrogen bond acceptor on that area should be avoided, whereas a hydrogen donor chemical function would be favourable. The latter agrees with our docking results achieved for the compounds **44** and **1x**–**9x,** which interact through the amide group by a hydrogen bond relation with the carboxylate function of Glu384 into the catalytic site of the enzyme.

Design of novel derivatives and molecular dynamics

Based on the information provided by the CoMFA and CoMSIA models, we have designed a series of compounds as leukotriene A_4 hydrolase inhibitors. Fig. 4 shows the proposed compounds with their predicted pIC_{50} values. The designed compounds **1x**–**8x** showed IC_{50} values in the nanomolar range, whereas the compounds **9x** and **10x** showed sub-nanomolar ranges in their IC_{50} values of the ability to inhibit LTA_4H. The compounds **1x**–**3x** had pIC_{50} values like the most active compound (compound **44**, Table S-I). Nonetheless, the compounds **4x**–**10x** exhibited better pIC_{50} values, and therefore, promising inhibitory activities over the enzyme. The best inhibitory profiles for the designed compounds **1x**–**10x** were obtained considering the following structural criteria: 1) incorporation of an aromatic thiazolopyridine or oxazolpyridine rings; 2) insertion of electropositive groups (chlorine contiguous to the methylene carbons) at positions 5 and 6 of the heterocycles (oxazolpyridine or thiazolopyridine) with the ability to increase the lipophilicity of this scaffold; 3) maintenance of the phenyl framework in order to obtain a certain distance between the thiazolopyridine and the bulky azabicyclooctane ring; 4) azabicyclooctane rings possessing at least one polar hydrogen bond acceptor chemical group, such as an amide or urea.

Then, we carried out a docking and molecular dynamics study of compounds **7x**, **9x** and **10x**. These derivatives had the highest predicted pIC_{50} values (9.942, 10.277 and 10.434, respectively). To examine the changes in the protein–inhibitor system, RMSD and RMSF trajectory analyzes were performed based on the backbone atoms. In protein–inhibitor complex MD simulations, *RMSD* measurements allow us to comment on the stability and the changes of protein and ligand. The strong interaction of the inhibitor with the enzyme makes the protein more stable. As seen in Fig. S-4A (Supplementary material), after 15 ns the system stabilized and continued with constant small shifts. Average *RMSD* values of 0.3, 0.24 and 0.19 nm were measured for LTA_4H–**7x**, LTA_4H–**9x** and LTA_4H–**10x** protein–ligand complexes, respectively. According to this result, the compound **10x** made the target LTA_4H enzyme more stable. *RMSF* corresponds to another analysis parameter that provides information about fluctuations and conformational changes of the protein–inhibitor complex. Residues with a high *RMSF* value indicate that they are more mobile, while those with a low *RMSF* value indicate that they are more stable. As seen in Fig. S-4B, the compound **9x** moved away from amino acids 290-310, its fluctuation in this region was higher than **7x** and **10x**. Therefore, the derivative **10x** was more stable interacting with the amino acids of the active site. The compound **10x** establishes a H bond with Tyr378.

The inhibitor binding modes and protein-inhibitor interaction diagrams of **7x**, **9x** and **10x** at the end of 100 ns are shown in Fig. 5, each one of them representing the change of the ligand at the catalytic site during the MD simulation process. Through its hydrogen atoms the amide group of the compound **7x** per-

forms two hydrogen bond interactions with Met270 and Gln143, respectively. On the other hand, Fig. 5 demonstrates that the compound **9x** carry out two hydrogen bond interactions between the oxygen atoms of both carbonyl functions of the amide groups at the azabicyclic moiety with Arg563, as well as an extra hydrogen bond interaction through the hydrogen atom between one of its amides with Pro266. Finally, the compound **10x** showed the ability to form a hydrogen bond interaction with Tyr378 and the amide function that bears in its structure. Although there were some changes according to the binding poses obtained from molecular docking, the compounds **7x**, **9x** and **10x** continued to interact with the LTA_4H catalytic site.

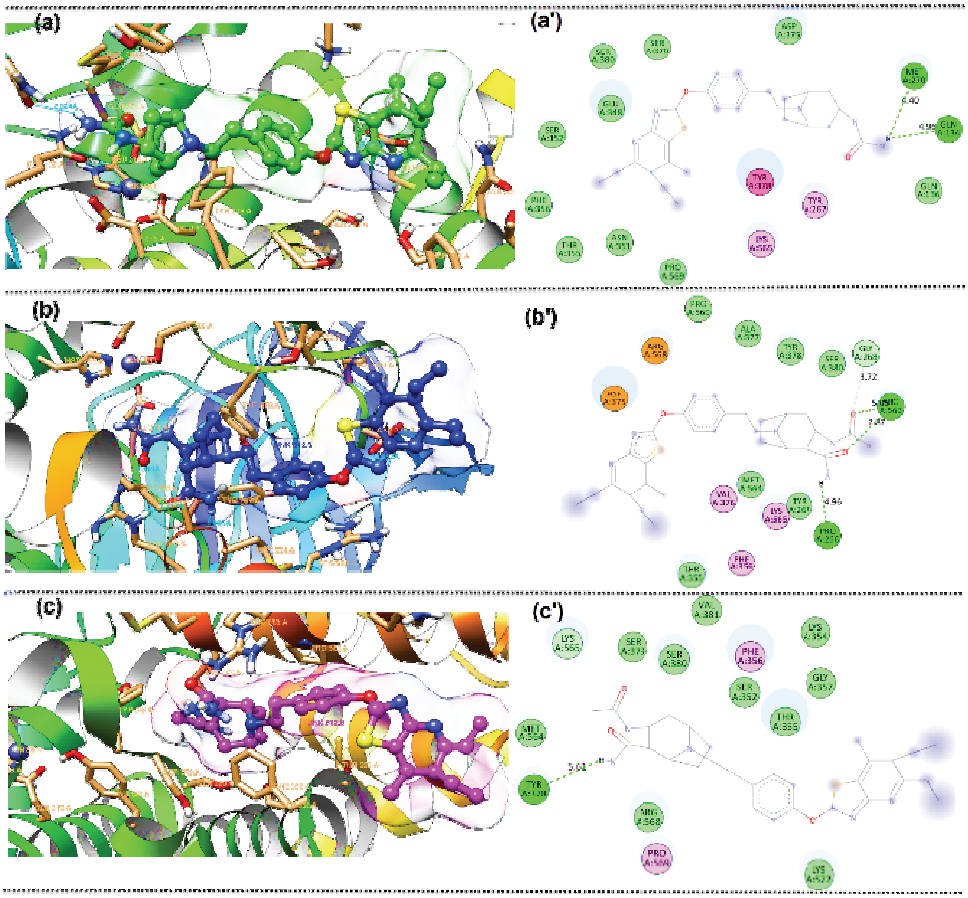

Fig. 5. Binding pose and protein-inhibitor schematic interactions of compound **7x** (a and a'), **9x** (b and b') and **10x** (c and c') in the LTA_4H catalytic site after 100 ns of molecular dynamics simulations.

Another important way to evaluate the protein–ligand interaction strength is by measuring the theoretical binding free energy. The latter parameter is obtained from the energy of the protein–inhibitor complex by subtracting the energies of the protein and ligand in single state, and the sum of the energies of van der Waals, electrostatic, polar solvation and solvent accessible surface area (*SASA*). As shown in Table I, the compounds **7x**, **9x** and **10x** gave mean BFE values of –205.40, –252.51 and –281.24 kJ/mol, respectively. In parallel with the *RMSD* and *RMSF* measurements, the compound **10x** showed the strongest interactions with the enzyme, corroborating its great potential as a LTA_4H inhibitor.

TABLE I. Results of MM-PBSA binding free energies (kJ/mol) between leukotriene A_4 hydrolase (LTA_4H) with compounds **7x**, **9x** and **10x**

Parameter	Complex		
	LTA_4H–**7x**	LTA_4H–**9x**	LTA_4H–**10x**
van der Waals	–121.43	–137.49	–174.21
Electrostatic	–542.03	–702.96	–235.00
Polar solvation	480.11	608.91	147.84
SASA	–22.06	–20.97	–19.86
Theoretical binding free energy	–205.40	–252.51	–281.24

Finally, considering the CoMFA, CoMSIA, docking studies and molecular dynamics simulation, we have summarised the structure–activity relationship in Fig. 6.

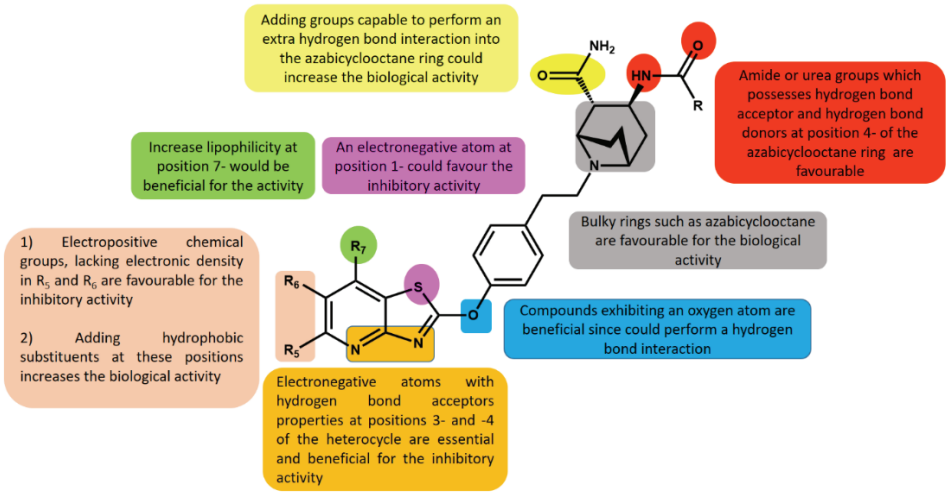

Fig. 6. Main structure–activity relationship found in this study. Substitution patterns were aimed to enhance the inhibitory activity over the human leukotriene A_4 hydrolase (LTA_4H).

CONCLUSION

Herein, we presented the construction of two QSAR models based on reported benzimidazole, benzoxazoles, benzothiazole and thiazolopyridine leukotriene A_4 hydrolase inhibitors (LTA_4H inhibitors). The models were externally validated. The best models presented q^2 values greater than 0.5. However, the CoMSIA model turned out to be superior, since it did not present outliers and exhibited a better external predictability coefficient (r^2_{test} = 0.851). Both models showed steric, electrostatic, hydrophobic and H-bond acceptor equilibria in the biological activity contribution. Using the information from the QSAR models, a new series of compounds were designed and presented (**1x**–**10x**). The predicted biological inhibitory activities for these new derivatives were high, exhibiting low IC_{50} in the nano- and sub-nanomolar ranges. Furthermore, the least active compound (**9**) and the most active compound (**44**), used to build the QSAR models, as well as **1x**-**10x** were subjected to docking assays with the human LTA_4H. In addition, the molecular dynamics simulations were carried out for the best compounds **7x**, **9x** and **10x**. The compound **10x** presented the best values of pIC_{50} (10.424), and the best binding profile according to the molecular dynamics and binding free energy calculations (-281.24 kJ/mol). Therefore, this compound represents an interesting lead compound for the development of new LTA_4H inhibitors.

SUPPLEMENTARY MATERIAL

Additional data and information are available electronically at the pages of journal website: https://www.shd-pub.org.rs/index.php/JSCS/article/view/11812, or from the corresponding author on request.

Acknowledgements. This work was financially supported by Conicyt/Fondecyt projects: Fondecyt de Iniciación en Investigación N° 11190145, Fondecyt grant 11130701; M.L thanks Beca Conicyt-PFCHA/Doctorado Nacional/2018-21180427; JRP acknowledge MRPF, GERR, GARP and CCRP. M.M. thanks to Fondecyt postdoctorado 2018 N° 3180408. All MD simulations presented here were carried out using resources provided by TÜBTAK (Turkish Scientific and Technological Research Council), ULAKBIM (Turkish Academic Network and Information Center) and TRUBA (High Performance and Grid Computing Center).

ИЗВОД

ДИЗАЈНИРАЊЕ БЕНЗИМИДАЗОЛА, БЕНЗОКСАЗОЛА, БЕНЗОТИАЗОЛА И ТИАЗОЛОПИРИДИНА КАО ИНХИБИТОРА ЛЕУКОТРИЕН A_4 ХИДРОЛАЗЕ, ПУТЕМ 3D-QSAR ДОКИНГА И МОЛЕКУЛСКЕ ДИНАМИКЕ

MARCOS LORCA[1], MARIO FAÚNDEZ[2], C. DAVID PESSOA-MAHANA[2], GONZALO RECABARREN-GAJARDO[2,3], BENJAMIN DIETHELM-VARELA[2], DANIELA MILLÁN[4], ISMAIL CELIK[5], MARCO MELLADO[6], ILEANA ARAQUE[1], JAIME MELLA[1,7] и JAVIER ROMERO-PARRA[8]

[1]Institute of Chemistry and Biochemistry, Faculty of Science, University of Valparaíso, Valpa¬ra¬íso 2360102, Chile, [2]Faculty of Chemistry and Pharmacy, Pontifical Catholic University of Chile, Santiago 7820436, Chile, [3]Interdisciplinary Center for Neurosciences, Pontifical Catholic Uni¬versity of Chile, Santiago 8330024, Chile, [4]Integrative Center for Biology and Applied Che¬mi¬stry, Bernardo O'Higgins University, Santiago 8370854, Chile, [5]Department of Pharma¬ceu¬ti¬cal Chemistry, Faculty of Pharmacy, Erciyes University, Kayseri 38039, Turkey, [6]Instituto de Inves¬tigación y Postgrado, Facultad de Ciencias de la Salud, Universidad Central de Chile, Santiago 8330507, Chile, [7]Chilean Pharmacopeia Research Center, University of Valparaíso, Valparaíso 2360134, Chile and [8]Department of Organic Chemistry u [8]Physical Chemistry, Faculty of Chemistry and Pharmaceutical Sciences, University of Chile, Santiago 8380544, Chile

Хумани ензим леукотриен A_4 хидролаза (LTA_4H) катализује биотрансформацију инактивног прекурсора леукотриена A_4 (LTA_4) у биоактивни леукотриен B4 (LTB_4), који изазива многе упалне одговоре у људском телу. Зато је селективна инхибиција овог ензима постале корисна стратегија за лечење разних болести као што су астма, алергијски ринитис, кардиоваскуларне болести и канцер. Овде приказујемо 3D-QSAR/ /CoMFA и CoMSIA студију на серији од 47 бензимидазола, бензоксазола, бензотиазола и тиазолопиридина за које се зна да су моћни LTA_4H инхибитори. Добијени су добри статистички параметри за најбољи модел (q^2 = 0,568, r^2_{ncv} = 0,891 и r^2_{test} = 0,851). Предложена је нова серија од 10 једињења која великом снагом могу да инхибирају леукотриен A_4 хидролазу. Сви дизајнирани инхибитори показују ниску IC_{50} у нано и субнаномоларним областима, када су оцењивани са 3D-QSAR моделима. Након тога, дизајнирани молекули, као и најмање и највише активна једињења су подвргнута студијама докинга и молекулске механике са LTA_4H. У закључку смо сажели темељиту релацију структуре и активности (SAR) за LTA_4H инхибиторе хетероцикличне структуре. Ови модели се могу искористити за рационално предлагање нових инхибитора.

(Примљено.27. априла, ревидирано 1. августа, прихваћено 18. августа 2022)

REFERENCES

1. J. Z. Haeggström, A. Rinaldo-Matthis, C. E. Wheelock, A. Wetterholm, *Biochem. Biophys. Res. Commun.* **396** (2010) 135 (https://doi.org/10.1016/j.bbrc.2010.03.140)
2. R. J. Snelgrove, *Thorax* **66** (2011) 550 (https://doi.org/10.1136/thoraxjnl-2011-200234)
3. N. Gueli, W. Verrusio, A. Linguanti, W. De Santis, N. Canitano, F. Ippoliti, V. Marigliano, M. Cacciafesta, *Arch. Gerontol. Geriatr.* **52** (2011) e36 (https://doi.org/10.1016/j.archger.2010.04.014)
4. T. D. Penning, L. J. Askonas, S. W. Djuric, R. A. Haack, S. S. Yu, M. L. Michener, G. G. Krivi, E. Y. Pyla, *Bioorg. Med. Chem. Lett.* **5** (1995) 2517 (https://doi.org/10.1016/0960-894X(95)00441-U)
5. N. L. Rao, P. J. Dunford, X. Xue, X. Jiang, K. A. Lundeen, F. Coles, J. P. Riley, K. N. Williams, C. A. Grice, J. P. Edwards, *J. Pharmacol. Exp. Ther.* **321** (2007) 1154 (https://doi.org/10.1124/jpet.106.115436)

6. W. Barchuk, J. Lambert, R. Fuhr, J.Z. Jiang, K. Bertelsen, A. Fourie, X. Liu, P.E. Silkoff, E.S. Barnathan, R. Thurmond, *Pulm. Pharmacol. Ther.* **29** (2014) 15 (https://doi.org/10.1016/j.pupt.2014.06.003)
7. E. Pontiki, D. Hadjipavlou-Litina, *Med. Res. Rev.* **28** (2008) 39 (https://doi.org/10.1002/med.20099)
8. P. R. Bernstein, *Am. J. Respir. Crit. Care. Med.* **157** (1998) S220 (https://doi.org/10.1164/ajrccm.157.6.mar-3)
9. L. V. Sonawane, S. B. Bari, *Acta Pharm. Sin., B* **45** (2010) 615 (http://www.ncbi.nlm.nih.gov/pubmed/20931764)
10. T. Sundarapandian, J. Shalini, S. Minky, A. Venkatesh, W. L. Keun, *Future Med. Chem*. **5** (2013) 27 (https://doi.org/10.4155/fmc.12.184)
11. V. M. Tanis, G. M. Bacani, J. M. Blevitt, C. C. Chrovian, S. Crawford, A. De Leon, A. M. Fourie, L. Gomez, C. A. Grice, K. Herman, *Bioorg. Med. Chem. Lett.* **22** (2012) 7504 (https://doi.org/10.1016/j.bmcl.2012.10.036)
12. C. A. Grice, K. L. Tays, B. M. Savall, J. Wei, C. R. Butler, F. U. Axe, S. D. Bembenek, A. M. Fourie, P. J. Dunford, K. Lundeen, *J. Med. Chem.* **51** (2008) 4150 (https://doi.org/10.1021/jm701575k)
13. D. R. Davies, B. Mamat, O. T. Magnusson, J. Christensen, M. H. Haraldsson, R. Mishra, B. Pease, E. Hansen, J. Singh, D. Zembower, *J. Med. Chem.* **52** (2009) 4694 (https://doi.org/10.1021/jm900259h)
14. M. Lorca, Y. Valdes, H. Chung, J. Romero-Parra, C.D. Pessoa-Mahana, J. Mella, *Int. J. Mol. Sci.* **20** (2019) 2510 (https://doi.org/10.3390/ijms20102510)
15. K. Roy, S. Kar, P. Ambure, *Chemometr. Intell. Lab. Syst.* **145** (2015) 22 (https://doi.org/10.1016/j.chemolab.2015.04.013)
16. R. Kumari, R. Kumar, A. Lynn, *J. Chem. Inf. Model.* **54** (2014) 1951 (https://doi.org/10.1021/ci500020m).